Collisionless relaxation of ion distributions downstream of laminar quasi-perpendicular shocks

L. Ofman,[1,2] M. Balikhin,[3] C. T. Russell,[4] and M. Gedalin[5]

Received 20 April 2009; revised 5 June 2009; accepted 12 June 2009; published 30 September 2009.

[1] Directed flow of incident ions provides the free energy which is redistributed in a shock among heated ions and electrons, accelerated particles, and magnetic compression. In low Mach number laminar shock the main channel of conversion is into downstream gyrating ions. Just behind the shock transition the ion distribution is substantially nongyrotropic, which results in spatially periodic variations of the ion pressure and, consequently, in time stationary downstream oscillations of the magnetic field. In the absence of significant level of nonstationarity, gyrotropization is due to the gyrophase mixing and slow. Theoretical analysis of the phenomenon and supporting hybrid simulations are presented. It is shown that these oscillations are more likely to be observed at low Mach number low β shocks, while at higher Mach numbers or higher β they may be obscured by waves crossing the shocks.

Citation: Ofman, L., M. Balikhin, C. T. Russell, and M. Gedalin (2009), Collisionless relaxation of ion distributions downstream of laminar quasi-perpendicular shocks, *J. Geophys. Res.*, *114*, A09106, doi:10.1029/2009JA014365.

1. Introduction

[2] Directed flow of incident ions provides all the energy which is to be redistributed by a collisionless shock among heated and accelerated particles, and compressed magnetic field. Relative efficiency of the conversion in each channel depends on the shock parameters, including Mach number, the angle between the shock normal and the upstream magnetic field, and the velocity distribution of the species in the incident flow. High Mach number shocks with no pickup ions are characterized by significant ion reflection [*Leroy et al.*, 1982; *Sckopke et al.*, 1983; *Burgess et al.*, 1989; *Sckopke et al.*, 1990]. Substantial number of pickup ions may result in main energy conversion into accelerated particles while leaving a small part for the heated body of the downstream ion distribution [*Zank et al.*, 1996; *Wang et al.*, 2008; *Decker et al.*, 2008]. In low Mach number shocks the field profile is expected to be stationary and one-dimensional [*Greenstadt et al.*, 1975; *Russell et al.*, 1982; *Farris et al.*, 1993], while there are no or almost no reflected ions, provided the upstream plasma is not too hot. In this case most part of the upstream ion energy goes into downstream heated ion distribution [*Thomsen et al.*, 1985].

[3] The magnetic field profile is closely related to the ion distributions in the shock front. Large-amplitude magnetic oscillations (overshoots and undershoots) downstream of a supercritical shock ramp have been shown to be due to the nongyrotropic part of the ion distribution [*Sckopke et al.*, 1983; *Scudder et al.*, 1986; *Burgess et al.*, 1989]. This nongyrotropy is provided by the reflected ions which cross again the ramp and appear as a gyrating beam downstream [*Leroy et al.*, 1982; *Burgess et al.*, 1989]. The pressure of this beam oscillates with the distance from the ramp [*Gedalin*, 1997], which, together with (at least) approximate constancy of the total pressure across the shock front, results in the magnetic field oscillations which are anticorrelated with the ion pressure variations. Reflected ions and nongyrotropy of the downstream distribution have been observed also for marginally critical shocks [*Sckopke et al.*, 1990]. Downstream ion distributions in low Mach number shocks (well below the critical Mach number) are widely believed to be nearly gyrotropic in the absence of reflected ions, and no overshoot-undershoot structure is expected to occur in such shocks. Observations [see *Greenstadt et al.*, 1975; *Russell et al.*, 1982; *Farris et al.*, 1993; *Russell et al.*, 2009], however, show that in addition to high-frequency (small scale) noise, there are large-scale waves on the downstream part of the magnetic profiles of such shocks. The polarization properties of these waves are similar to those of compressional magnetosonic waves [*Russell et al.*, 2009], and often they are interpreted as propagating waves. Yet, a comprehensive analysis of a single low Mach number shock [*Zilbersher et al.*, 1998] has shown that such magnetic oscillations can be stationary in the shock frame, and the shock itself is one-dimensional. Interpretation of these oscillations in terms of damping soliton [*Sagdeev*, 1966; *Kennel and Sagdeev*, 1967; *Kennel et al.*, 1985] is not consistent with the shock parameters. Recently, it has been shown [*Balikhin et al.*, 2008] that in a very low Mach number, very low β shock, stationary oscillations of the downstream magnetic field arise owing to the gyration of the downstream ion distribution as a whole. Here we generalize this approach

[1]CUA and NASA GSFC, Greenbelt, Maryland, USA.
[2]Department of Geophysics and Planetary Sciences, Tel Aviv University, Tel Aviv, Israel.
[3]ACSE, University of Sheffield, Sheffield, UK.
[4]Institute of Geophysics and Planetary Physics, University of California, Los Angeles, California, USA.
[5]Department of Physics, Ben-Gurion University, Beer-Sheva, Israel.

Copyright 2009 by the American Geophysical Union.
0148-0227/09/2009JA014365

and show that the effect is of purely kinetic nature, and is due to the gyration of the ions crossing the shock front.

[4] The directed flow energy of incident ions is effectively converted at the quasi-perpendicular collisionless shock front into the energy of broadened downstream distribution in a complex process. First, the ions crossing the shock start to gyrate. This gyration eventually results in the effective broadening of the ion distribution function. A part of the broadening occurs right after crossing the ramp where a substantially nongyrotropic distribution forms. However, main broadening occurs only after gyrophase mixing and resulting gradual gyrotropization of the ion distribution. Shock front nonstationarity may substantially speed up the gyrophase mixing. Wave-particle interaction, either due to the instabilities in the downstream region or due to waves crossing the shock from the upstream, smooths out irreversibly to also gyrotropize and shape the heated ion distribution. In a nonstationary shock the processes cannot be separated, since the time-dependent fields in the shock front efficiently play the role of the wavefields. In a stationary shock, however, one may expect that the two processes are separated in time and in space (gyration starts immediately upon crossing the ramp, followed by the collisionless gyrophase mixing, while the wave-particle interaction becomes noticeable farther downstream from the ramp). If the level of fluctuations is low, there should be a wide region behind the ramp, where wave-particle interaction is not sufficiently fast to shape the distributions, and the purely collisionless shaping of the ion distribution can be observed. This process consists of prompt formation of a nongyrotropic distribution and subsequent gradual gyrotropization due to the collisionless gyrophase mixing. In this paper we develop a simple analytical theory of the collisionless relaxation due to ion gyration and gyrophase mixing and support it with 1D hybrid simulations. We show that the downstream ion pressure becomes spatially periodic, which in turn results in periodic oscillations of the magnetic field behind the ramp. These oscillations decay with the gyrophase mixing. The effect depends on the shock parameter, like the Mach number, the angle between the shock normal and the upstream magnetic field, and the upstream ion β.

2. Theory

[5] The ramp width of a quasi-perpendicular collisionless shock is substantially smaller than the upstream ion convective gyroradius [*Russell et al.*, 1982], so that a typical ion crossing a ramp is not deflected significantly by the magnetic field, while at the same time being decelerated by the cross-shock potential. For simplicity we shall describe a collisionless shock as a discontinuity. We do not lose substantial physics in this way while allowing analytical consideration. Let the shock normal be along the x axis, and the noncoplanarity direction be along y. The shock front (the discontinuity) is at $x = 0$. We denote the upstream and downstream magnetic field as follows: $\boldsymbol{B}_u = B_u(\cos\theta, 0, \sin\theta)$ and $\boldsymbol{B}_d = B_u(\cos\theta, 0, R\sin\theta)$. We shall call R the magnetic compression. Let the potential jump on the discontinuity be $e\varphi = s(m_i v_u^2/2)$, where m_i is the ion mass and v_u is the upstream plasma flow. We shall also denote $v_h = v_T/v_u$ the dimensionless upstream ion thermal velocity. It is related to $\beta_i = 8\pi n_u T_u/B_u^2$ as follows: $v_h^2 = \beta_i/2M^2$, where the Alfvénic Mach number $M = v_u/v_A$, $v_A^2 = B_u^2/4\pi n_u m_i$.

[6] With all above taken into account, an ion, which enters the shock with the velocity $\boldsymbol{V} = v_u(v_x, v_y, v_z)$, leaves it with the velocity $\boldsymbol{U} = v_u(u_x, u_y, u_z)$ such that

$$u_x = \sqrt{v_x^2 - s}, \quad u_y = v_y, \quad u_z = v_z \tag{1}$$

where we assume that all ions are able to overcome the potential. In what follows all ion velocities are given in the shock (normal incidence) frame.

[7] The ion equation of motion behind the shock is

$$m_i \dot{\boldsymbol{W}} = e\boldsymbol{E} + e\boldsymbol{W} \times \boldsymbol{B}_d/c \tag{2}$$

where $\boldsymbol{E} = (0, v_u B_u \sin\theta/c, 0)$, and $\boldsymbol{W}$ is the downstream ion velocity. Using normalized variables, $\boldsymbol{W} = v_u(w_x, w_y, w_z)$, one has

$$\dot{w}_x = R w_y \sin\theta \tag{3}$$

$$\dot{w}_y = \sin\theta + w_z \cos\theta - R w_x \sin\theta \tag{4}$$

$$\dot{w}_z = -w_y \cos\theta \tag{5}$$

where $\dot{\boldsymbol{w}} = d\boldsymbol{w}/d\tau$ and $\tau = \Omega_u t = (eB_u/m_i c)t$. We need only w_x which takes the form

$$w_x = V_d + V_g \sin(b_d \tau + \psi) \tag{6}$$

$$V_d = k_1^2 u_x + k_1 k_2 u_z + \frac{k_2^2}{R} \tag{7}$$

$$b_d = \sqrt{R^2 \sin^2\theta + \cos^2\theta}, \quad k_1 = \cos\theta/b_d, \quad k_2 = R\sin\theta/b_d \tag{8}$$

$$V_g = k_2\left[u_\perp^2 + u_y^2\right]^{1/2}, \quad \tan\psi = u_\perp/u_y \tag{9}$$

$$u_\perp = k_2(u_x - 1/R) - k_1 u_z \tag{10}$$

Respectively, the expression for the ion coordinate along the shock front reads

$$X = \frac{x}{(v_u/\Omega_u)} = V_d\tau + \frac{V_g}{B_d}[\cos\psi - \cos(B_d\tau + \psi)] \tag{11}$$

Once the equation $x = x(u_x, u_y, u_z, \tau)$ is inverted to obtain $\tau = \tau(x, u_x, u_y, u_z)$ (this function may be multivalued) we will have $w_{x,i} = w_{x,i}(x, u_x, u_y, u_z)$, where subscript i shows that there may be several solutions. Physically that means that an ion trajectory can cross the plane x = const more than one time if the gyration velocity V_g exceeds the drift velocity V_d.

[8] The shock is stationary if the pressure balance $p_{xx} + B^2/8\pi = \text{const}$ is satisfied everywhere. It is therefore natural to analyze the behavior of the total ion pressure tensor

$$p_{xx} = m_i \int f(\boldsymbol{w}) w_x^2 d^3\boldsymbol{w} \tag{12}$$

It should be noted that the total pressure tensor includes the thermal pressure and the dynamic pressure, $p_{xx} = p_{ram,xx} + p_{th,xx}$, where

$$p_{dyn,xx} = n m_i \langle w_x \rangle^2, \qquad n\langle w_x \rangle = \int f(\boldsymbol{w}) w_x d^3\boldsymbol{w} \tag{13}$$

$$p_{th,xx} = m_i \int f(\boldsymbol{w})(w_x - \langle w_x \rangle)^2 d^3\boldsymbol{w} \tag{14}$$

It is easy to see that ion number conservation requires that

$$f_0(\boldsymbol{v})|v_x| d^3\boldsymbol{v} = f(\boldsymbol{w})|w_x| d^3\boldsymbol{w} \tag{15}$$

so that the expression for the ion pressure reduces to the following

$$p_{xx} = \sum_i m_i \int f_0(\boldsymbol{v})|v_x||w_{x,i}| d^3\boldsymbol{v} \tag{16}$$

The derived expression is valid for any ratio V_g/V_d. Here we shall consider for simplicity the case of a cold upstream plasma, which means $u_x = \sqrt{1-s}$, $u_y = u_z = 0$, and

$$V_g = k_2^2 \left| \sqrt{1-s} - 1/R \right|, \quad V_d = k_1^2 \sqrt{1-s} + k_2^2/R \tag{17}$$

When $V_g < V_d$ there is only one solution $w_x = w_x(x, u_x, u_y, u_z)$. For $V_g \ll V_d$ one has approximately $\tau = X/V_d$ and

$$w_x = V_d - V_g \sin(b_d X/V_d) \tag{18}$$

$$p_{xx} = n_u m_i v_u^2 \left[V_d - V_g \sin(b_d X/V_d) \right] \tag{19}$$

For a cold beam the expression for the pressure takes the form

$$p_{xx} = \sum_i n_u m_i v_u |W_{x,i}| \tag{20}$$

and approximately

$$p_{xx} = n_u m_i v_u^2 \left| V_d - V_g \sin(b_d X/V_d) \right| \tag{21}$$

[9] Thus, the total ion pressure becomes a periodic function of the coordinate behind the ramp. Stationarity of the shock implies pressure balance

$$p_{i,xx} + p_{e,xx} + \frac{B^2}{8\pi} = \text{const} \tag{22}$$

throughout. For a low electron pressure that means that the magnetic pressure and, therefore, the magnetic field magnitude, should be also periodic. The spatial period of oscillations is $L_o = 2\pi L_u V_d/b_d \sim 2\pi L_u/R^2$.

[10] If the ion distribution is not cold, each ion drifts with its own drift velocity V_d and gyrates with its own gyration velocity V_g. The difference in V_d for different ions results in a gradual phase mixing. The length scale for this mixing may be easily estimated using equation (7) which shows that the spread in the drift velocities is $\delta V_d \sim k_1 k_2 v_h$. The number of oscillations, occurring before the distribution is smoothed out owing to the gyrophase mixing, is given by $V_d/\delta V_d \sim k_2/k_1 R v_h \sim\sim R/v_h \cos\theta$.

[11] The above analysis shows that the magnetic field profile should exhibit coherent oscillations behind the ramp. These oscillations will alter the ion motion, which cannot be taken into account in our analytical study. Given these magnetic oscillations are rather weak, the applied approximation of the constant downstream magnetic field is expected to be quite satisfactory to elucidate the physics of the phenomenon.

[12] Complete analytical derivation of the downstream ion pressure as a function of position is impossible since it requires inversion of the expression (11). Yet some qualitative conclusions regarding dependence of the bulk gyration and gyrophase mixing on the shock parameters can be readily derived from the mathematical development above. For given angle θ, magnetic compression R, and cross-shock potential s, the larger is $v_T/v_u = \sqrt{\beta/2M^2}$, the larger is the typical ratio V_g/V_d of the gyration velocity to the drift velocity downstream. For sufficiently large β/M^2 a part of the ions start making loops, thus enhancing gyrophase mixing. For given β, θ, s, and M, higher magnetic compression R would increase the ratio V_g/V_d thus also enhancing gyrophase mixing. Since R, s, and M are interrelated, the most reliable conclusion would be that increasing β with the other shock parameters intact would make the pressure oscillations less pronounced and faster damping. Respectively, a decrease of the angle θ in the quasi-perpendicular case would decrease V_d and enhance gyrophase mixing for nonzero β.

3. Simulations

[13] A more sophisticated analytical treatment is hardly possible since there is no detailed theory for the fields in the shock profile and the equations of motion cannot be solved, in general. Instead we performed 1-D high-resolution (less than $0.1(c/\omega_{pi})$) hybrid simulation with massless electrons and protons modeled as particles. The 1D hybrid code is based on the code developed initially by *Winske and Omidi* [1993], and later modified by *Ofman et al.* [2001]. The hybrid model included more than 2000 grid cells with 1600 particles per cell. The shock was setup by launching a beam of protons and imposing a reflecting boundary conditions at one end of the simulation region. The reflected proton beam produces the shock by the interaction with the incoming beam. The parameters for the simulated shocks were chosen so that it would be possible to compare (approximately) the results of the numerical analysis with observations. The first two shocks are similar to the one described by *Balikhin et al.* [2008], while the third and the fourth are similar to the

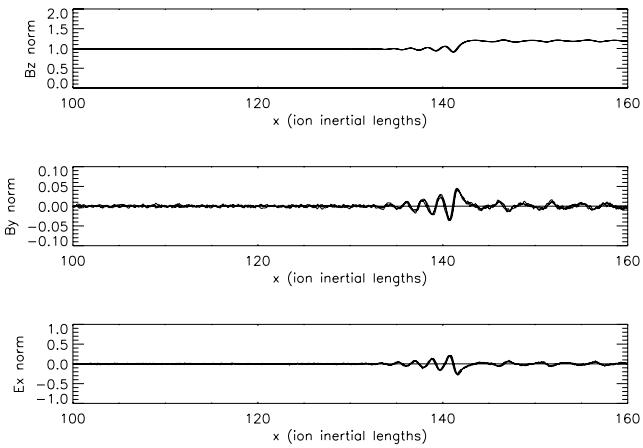

Figure 1. Four successive profiles of the main magnetic field B_z, noncoplanar magnetic field B_y, and electric field E_x (all normalized), overplotted with the same spatial shift for each two. The shock is stationary. Shock parameters are $\beta_i = \beta_e = 0.1$, $\theta = 80°$, $M = 1.22$.

second and the first shock in Figure 2 of *Farris et al.* [1993]. Figure 1 shows four profiles of the fields obtained in the run with $\beta_i = \beta_e = 0.1$ and $\theta = 80°$, for times t, $t + \Delta t$, $t + 2\Delta t$, and $t + 3\Delta t$, where Δt is a time interval, specific for each shock, usually $5/\omega_{pi}$. The later profiles are spatially shifted by l, $2l$, and $3l$, respectively, to fit. The spatial shift, l, is also specific for each shock and was typically $\sim 5(c/\omega_{pi})$. The shock velocity in the simulation frame is $V_{shock} = l/\Delta t$, while the upstream plasma velocity, which determines the Mach number, is $v_u = V_{plasma} + V_{shock}$, where V_{plasma} is the plasma injection speed along the shock normal at the box boundary. The shock is stationary and moving with a constant velocity. The fields are normalized as follows: B_z/B_u, B_y/B_u, $(E_x/B_u)(c/v_A)$. Figure 2 shows the moments of the ion distribution in the normal incidence frame: density n/n_u, hydrodynamical velocity v_x/v_A, and p_{xx}/p_0, where $p_0 = n_u(m_i v_u^2 + T_u) = n_u m_i v_A^2(M^2 + \beta_i/2)$. The Mach number for this shock is $M = 1.22$. The upper panel shows the density and the ion velocity along the

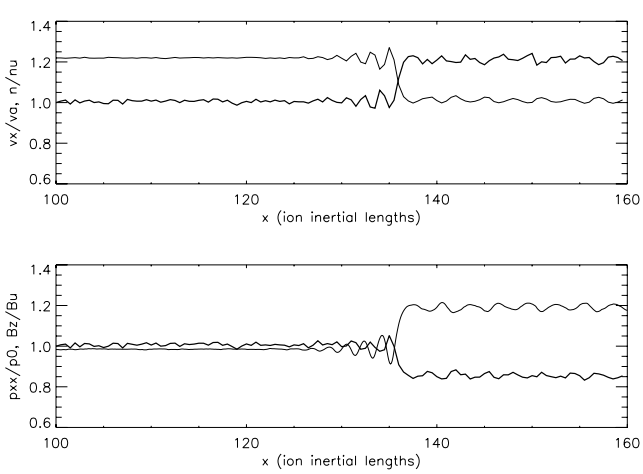

Figure 2. (top) Density n/n_u (thick line) and velocity v_x/v_A; (bottom) p_{xx}/p_0 (thick line) and B_z/B_u. All quantities are shown in the normal incidence frame. Shock parameters are $\beta_i = \beta_e = 0.1$, $\theta = 80°$, $M = 1.22$.

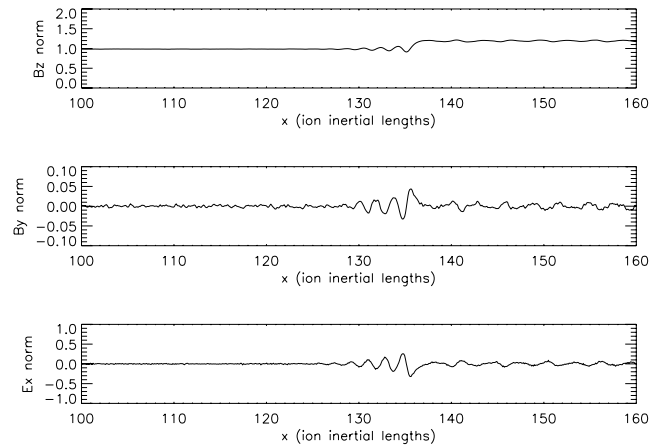

Figure 3. Fields in the normal incidence frame. Shock parameters are $\beta_i = \beta_e = 0.1$, $\theta = 80°$, $M = 1.22$.

shock normal. The bottom panel shows the total ion pressure (dynamic + thermal), along with the magnetic field (thin line). It is clearly seen that the ion pressure is spatially periodic with the period of about $3(c/\omega_{pi})$. The cold plasma approximation gives a spatial period that is twice larger than that obtained in the simulations. The discrepancy is due to the shock width, which is nonzero, and due to $V_g \sim V_d$. The ion pressure oscillations anticorrelate with the magnetic field oscillations. The latter slowly damp into the downstream region, with the damping length much larger than the period. The fields in the normal incidence frame are shown in Figure 3. The width of the main ramp is $\approx (c/\omega_{pi})$, which is consistent with the theoretical predictions by *Gedalin* [1998]. The wavelength of the precursor oscillations is twice as large, and is consistent with the theoretical description as a decaying train of nonlinear magnetosonic waves [*Sagdeev*, 1966; *Kennel and Sagdeev*, 1967]. The noncoplanar magnetic field is quite small and may be neglected. The cross-shock electric field is quite high, and the maximum potential drop (at the ramp) can be estimated as $(eV/m_i V_u^2/2) \approx 2 \cdot 0.5(eB_u/m_i c)(v_A/c)0.5(c/\omega_{pi})(1/M^2 v_A^2) \approx 0.5/M^2$. Overall, the similarity of the simulated shock to the one from *Balikhin et al.* [2008] is very good.

[14] Figure 4 shows the moments of the ion distribution for a similar shock with $\theta = 77°$ and $\beta_i = \beta_e = 0.2$. The shock is stationary. The Mach number is $M = 1.48$. The corresponding fields are shown in Figure 5. The two shocks are very similar, with the only noticeable difference in small-scale fluctuations of the fields, apparently because of larger β.

[15] In order to follow the changes in the distribution function of the ions throughout the shock front we present in Figure 6 the filled contour plot of the distribution in $v_x - v_y$ plane for three positions: $x = 120$ is at the upstream edge of the upstream precursor, $x = 132$ is within the precursor close to the ramp, while $x = 146$ is downstream. The complete movie, better showing the variations of the distribution shape, in particular, transition to a nongyrotropic gyrating distribution at the ramp, can be found in Animation 1.[1]

[1]Animations 1–3 are available in HTML.

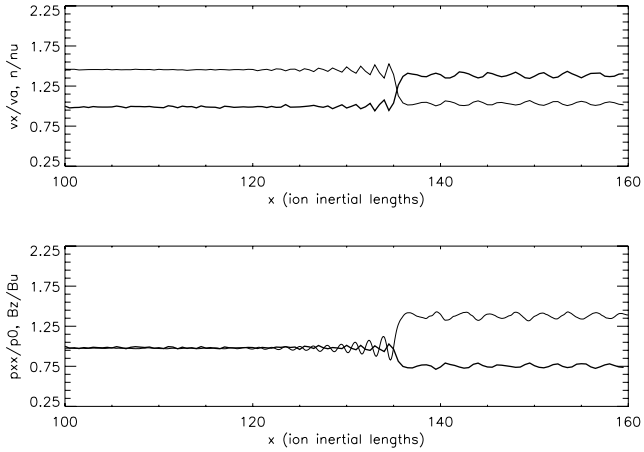

Figure 4. (top) Density n/n_u (thick line) and velocity v_x/v_A; (bottom) p_{xx}/p_0 (thick line) and B_z/B_u. All quantities are shown in the normal incidence frame. Shock parameters are $\beta_i = \beta_e = 0.2$, $\theta = 77°$, $M = 1.48$.

[16] A shock with a higher Mach number, $M = 2.2$, and higher $\beta = 1$ (compare with the second shock in Figure 2 of *Farris et al.* [1993]), is shown in Figure 7. The shock is still quite stationary, although the small-scale fluctuations of the fields are more intense. The corresponding distributions and fields are shown in Figures 8 and 9, respectively. The pressure and magnetic field oscillations are still visible, although they are less pronounced and more irregular, and damp into downstream much faster than in the previous cases. The magnetic precursor disappears and the electric field has a single peak inside the ramp of the width $\approx 2(c/\omega_{pi})$.

[17] The distributions across the shock are shown in Figure 10, in the format similar to that of Figure 6. The complete movie, better showing the variations of the distribution shape, in particular, transition to a nongyrotropic gyrating distribution at the ramp, can be found in Animation 2.

[18] Finally (Figure 11), we present the results for an oblique shock with $M = 1.5$, $\theta = 58°$ and $\beta = 0.07$ (compare with the first shock in Figure 2 of *Farris et al.* [1993]). This shock is also found to be stationary. Despite the low Mach number and low β, the downstream oscillatory structure is barely seen because of the faster gyrophase mixing for smaller angles.

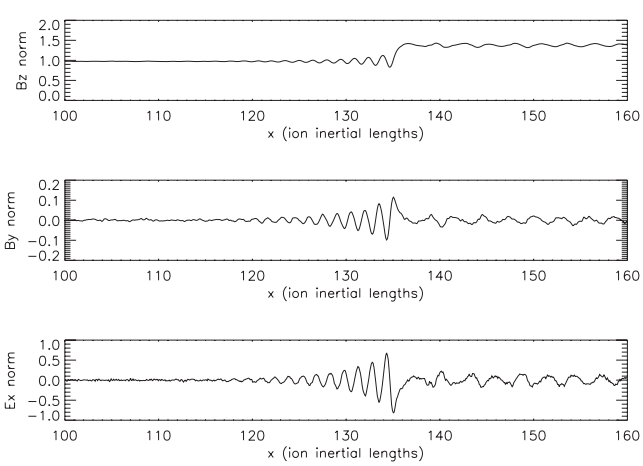

Figure 5. Fields in the normal incidence frame. Shock parameters are $\beta_i = \beta_e = 0.2$, $\theta = 77°$, $M = 1.48$.

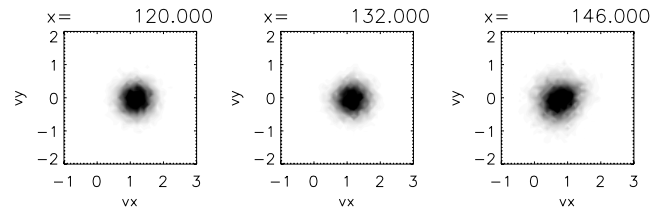

Figure 6. Distribution in $v_x - v_y$ plane for three positions: (left) $x = 120$ is at the upstream edge of the precursor, i.e., gyrotropic distribution, (middle) $x = 132$ is within the precursor near the ramp, i.e., almost gyrotropic distribution, (right) $x = 146$ is in the downstream, i.e., elongated nongyrotropic.

[19] The distributions across the shock are shown in Figure 12, in a format similar to that of Figure 6. The complete movie, better showing the variations of the distribution shape, in particular, transition to a nongyrotropic gyrating distribution at the ramp, can be found in Animation 3.

[20] In all low β cases above there is a precursor upstream of the ramp. The precursor is longer for lower angles θ. Similar to what happens downstream, in these precursors the magnetic field and the density are in the same phase, while the ion pressure is in the opposite phase. However, the mechanism is different: while in the downstream region the ion distributions gyrate around the nearly constant drift velocity, in the upstream region it is the drift velocity which follows the magnetic field, and the dominant term in the ion pressure is $nmv_d^2 \propto 1/n$, since nv_d = const. There is no precursor in the simulated $\beta = 1$ shock, which may be related

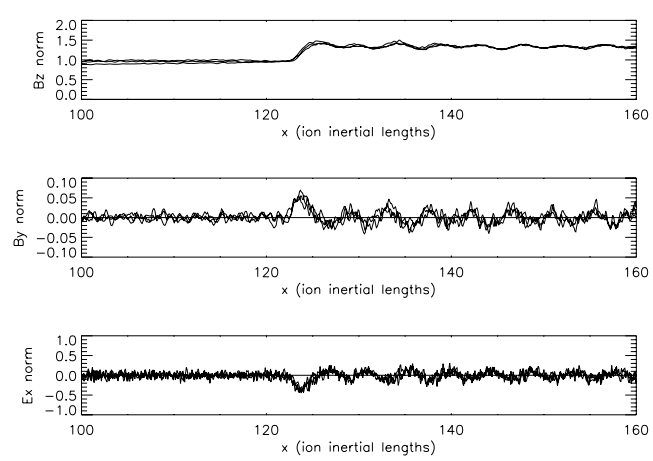

Figure 7. Four successive profiles of the main magnetic field B_z, noncoplanar magnetic field B_y, and electric field E_x (all normalized), overplotted with the same spatial shift for each two. The shock is stationary. Shock parameters are $\beta_i = \beta_e = 1$, $\theta = 73°$, $M = 2.2$.

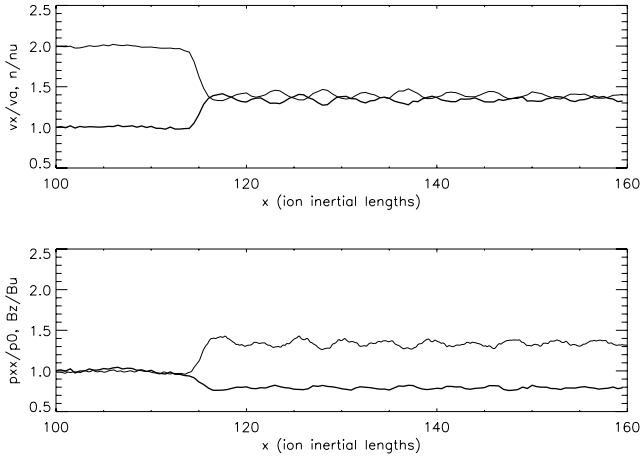

Figure 8. (top) Density n/n_u (thick line) and velocity v_x/v_A; (bottom) p_{xx}/p_0 (thick line) and B_z/B_u. All quantities are shown in the normal incidence frame. Shock parameters are $\beta_i = \beta_e = 1$, $\theta = 73°$, $M = 2.2$.

to different dispersion properties of the waves in low and high β plasmas [*Sagdeev*, 1966; *Kennel and Sagdeev*, 1967].

4. Discussion

[21] Ion gyration and the formation of nongyrotropic downstream distributions is a natural result of the ion dynamics in the shock front, whether it is a low Mach number or a high Mach number shock. The nongyrotropy of the distribution inevitably leads to spatially dependent ion pressure. In the case of a laminar shock where nonstationarity is not sufficient to smear out the nongyrotropy the pressure becomes almost spatially periodic. In laminar shocks the pressure balance has to be maintained throughout the shock, thus variations of the ion pressure should be accompanied with variations of electron pressure and magnetic pressure. If the electron heating is substantially weaker than the ion heating, then the magnetic oscillations should balance the oscillating ion pressure. These oscillations decay with gyrotropization of the ion distribution which is

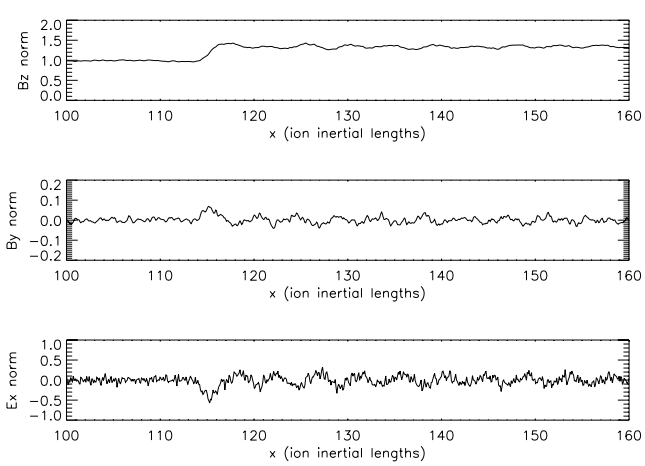

Figure 9. Fields in the normal incidence frame. Shock parameters are $\beta_i = \beta_e = 1$, $\theta = 73°$, $M = 2.2$.

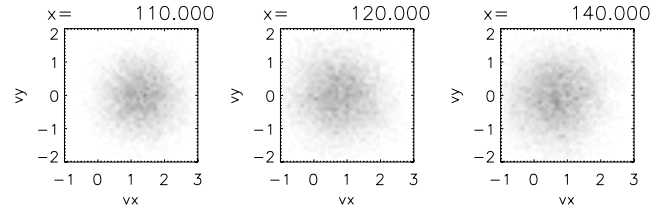

Figure 10. Distribution in v_x - v_y plane for three positions: (left) $x = 110$ is in the upstream, i.e., gyrotropic, (middle) $x = 120$ is in the downstream near the ramp, i.e., nongyrotropic, but nongyrotropy less pronounced than in the low β case, (right) $x = 140$ is well in the downstream, i.e., nongyrotropy substantially smoothed out owing to gyrophase mixing.

primarily because of the collisionless gyrophase mixing. The amplitude of the magnetic field oscillations in the low Mach number shocks is small. Variations of the main magnetic field component B_z are accompanied with the variations of the noncoplanar magnetic field B_y. The amplitude of the latter $\Delta B_y \ll \Delta B_z$, while the phase difference is $\pi/2$. In the usual minimal variance analysis of observations these oscillations would be identified as elliptically polarized with a large ratio of components, that is, almost linearly polarized waves. In this case determination of the "direction of propagation" would be extremely difficult. In these conditions any noticeable admixture of waves propagating through the shock would spoil identification of the stationary pattern related to the collisionless relaxation. Yet the stationary magnetic oscillations accompanying nongyrotropic ion distributions should be observed in most laminar shocks, although best conditions for such observations would require low upstream wave activity and low upstream ion temperature.

[22] It is worth mentioning that the mechanism of collisionless relaxation in laminar shocks is not different physically from the mechanism of the overshoot formation in supercritical shocks, where the reflected ions play the role

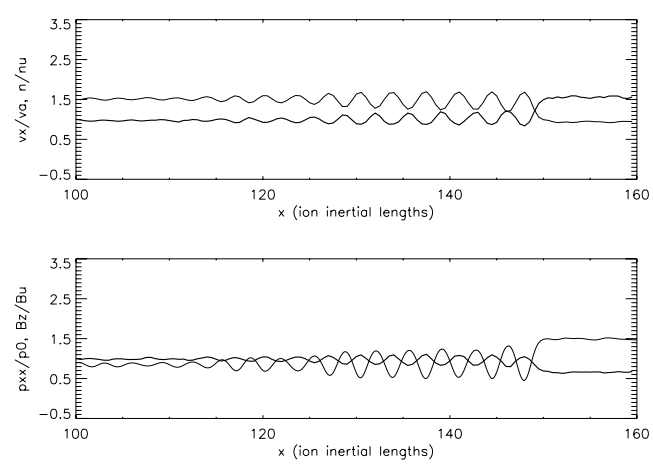

Figure 11. (top) Density n/n_u (thick line) and velocity v_x/v_A; (bottom) p_{xx}/p_0 (thick line) and B_z/B_u. All quantities are shown in the normal incidence frame. Shock parameters are $\beta_i = \beta_e = 0.07$, $\theta = 58°$, $M = 1.5$.

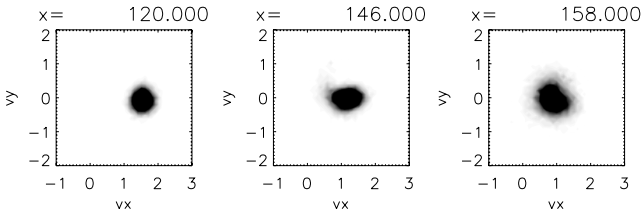

Figure 12. Distribution in v_x - v_y plane for three positions: (left) x = 120 is in the beginning of the precursor - almost gyrotropic, centered at shifted drift velocity, (middle) x = 146 is deep within the precursor, near the ramp - substantial nongyrotropy develops, centered around shifted drift velocity, (right) x = 158 is in the downstream - gyrophase mixing already partially smoothed out the nongyrotropy.

of the gyrating ion distribution and produce a similar train of magnetic oscillations behind the ramp.

5. Conclusions

[23] In summary, we have shown analytically and supported by hybrid simulations that (1) the gyration of the downstream ion distribution should produce the oscillations of ion pressure and, consequently, oscillations of the downstream magnetic field; (2) the downstream distribution is slowly smoothed out owing to the collisionless gyrophase mixing so that the oscillations gradually damp; (3) gyrophase mixing is faster for higher initial thermal velocities, higher magnetic compression, and smaller angles between the shock normal and upstream magnetic field; (4) collisionless relaxation due to gyrophase mixing can be observed at most laminar shocks.

[24] The simulated profiles of the magnetic fields are in good agreement with earlier observations [*Farris et al.*, 1993; *Balikhin et al.*, 2008], although it is not known to what extent the observed shocks are one-dimensional and stationary. The process of collisionless relaxation occurs even in high Mach number shocks where, however, mixing may occur at the scale of one ion gyroperiod.

[25] **Acknowledgments.** M.B. and M.G. acknowledge support by the Royal Society and ISSI. M.G. was partially supported by ISF grant 275/07. M.B. is grateful to STFC for support of the research based on VEX magnetometer data. M.G. acknowledges support by the University of Sheffield. L.O. would like to acknowledge support by NASA grants NNX08AV88G and NNX08AF85G.

[26] Wolfgang Baumjohann thanks Gary Zank and another reviewer for their assistance in evaluating this paper.

References

Balikhin, M. A., T. L. Zhang, M. Gedalin, N. Y. Ganushkina, and S. A. Pope (2008), Venus express observes a new type of shock with pure kinematic relaxation, *Geophys. Res. Lett.*, *35*, L01103, doi:10.1029/2007GL032495.

Burgess, D., W. P. Wilkinson, and S. J. Schwartz (1989), Ion distributions and thermalization at perpendicular and quasi-perpendicular supercritical collisionless shocks, *J. Geophys. Res.*, *94*, 8783–8792, doi:10.1029/JA094iA07p08783.

Decker, R. B., S. M. Krimigis, E. C. Roelof, M. E. Hill, T. P. Armstrong, G. Gloeckler, D. C. Hamilton, and L. J. Lanzerotti (2008), Mediation of the solar wind termination shock by non-thermal ions, *Nature*, *454*, 67–70, doi:10.1038/nature07030.

Farris, M. H., C. T. Russell, and M. F. Thomsen (1993), Magnetic structure of the low beta, quasi-perpendicular shock, *J. Geophys. Res.*, *98*, 15,285–15,294.

Gedalin, M. (1997), Ion dynamics and distribution at the quasiperpendicular collisionless shock front, *Surv. Geophys.*, *18*, 541–566.

Gedalin, M. (1998), Low-frequency nonlinear stationary waves and fast shocks: Hydrodynamical description, *Phys. Plasmas*, *5*, 127–132, doi:10.1063/1.872681.

Greenstadt, E. W., F. L. Scarf, C. T. Russell, V. Formisano, and M. Neugebauer (1975), Structure of the quasi-perpendicular laminar bow shock, *J. Geophys. Res.*, *80*, 502–514, doi:10.1029/JA080i004p00502.

Kennel, C., and R. Sagdeev (1967), Collisionless shock waves in high β plasmas, *J. Geophys. Res.*, *72*, 3327–3341.

Kennel, C. F., J. P. Edmiston, and T. Hada (1985), A quarter century of collisionless shock research, in *Collisionless Shocks in the Heliosphere: A Tutorial Review*, *Geophys. Monogr. Ser.*, vol. 34, edited by R. G. Stone and B. T. Tsurutani, pp. 1–36, AGU, Washington D. C.

Leroy, M. M., D. Winske, C. C. Goodrich, C. S. Wu, and K. Papadopoulos (1982), The structure of perpendicular bow shocks, *J. Geophys. Res.*, *87*, 5081–5094.

Ofman, L., A. Viñas, and S. P. Gary (2001), Constraints on the O^{+5} anisotropy in the solar corona, *Astrophys. J.*, *547*, L175–L178, doi:10.1086/318900.

Russell, C., M. Hoppe, W. Livesey, and J. Gosling (1982), Isee-1 and-2 observations of laminar bow shocks: Velocity and thickness, *Geophys. Res. Lett.*, *9*, 1171–1174.

Russell, C. T., L. K. Jian, X. Blanco-Cano, and J. G. Luhmann (2009), Stereo observations of upstream and downstream waves at low mach number shocks, *Geophys. Res. Lett.*, *36*, L03106, doi:10.1029/2008GL036991.

Sagdeev, R. Z. (1966), Cooperative phenomena and shock waves in collisionless plasmas, *Rev. Plasma Phys.*, *4*, 23.

Sckopke, N., G. Paschmann, S. J. Bame, J. T. Gosling, and C. T. Russell (1983), Evolution of ion distributions across the nearly perpendicular bow shock: Specularly and non-specularly reflected-gyrating ions, *J. Geophys. Res.*, *88*, 6121–6136.

Sckopke, N., G. Paschmann, A. L. Brinca, C. W. Carlson, and H. Luehr (1990), Ion thermalization in quasi-perpendicular shocks involving reflected ions, *J. Geophys. Res.*, *95*, 6337–6352, doi:10.1029/JA095iA05p06337.

Scudder, J. D., T. L. Aggson, A. Mangeney, C. Lacombe, and C. C. Harvey (1986), The resolved layer of a collisionless, high beta, supercritical, quasi-perpendicular shock wave: 1. Rankine-Hugoniot geometry, currents, and stationarity, *J. Geophys. Res.*, *91*, 11,019–11,052, doi:10.1029/JA091iA10p11019.

Thomsen, M. F., J. T. Gosling, S. J. Bame, and M. M. Mellott (1985), Ion and electron heating at collisionless shocks near the critical Mach number, *J. Geophys. Res.*, *90*, 137–148, doi:10.1029/JA090iA01p00137.

Wang, L., R. P. Lin, D. E. Larson, and J. G. Luhmann (2008), Domination of heliosheath pressure by shock-accelerated pickup ions from observations of neutral atoms, *Nature*, *454*, 81–83, doi:10.1038/nature07068.

Winske, D., and N. Omidi (1993), *Computer Space Plasma Physics: Simulation Techniques and Sowftware*, edited by H. Matsumoto and Y. Omura, pp. 103–160, Terra Sci., Tokyo.

Zank, G., H. Pauls, I. Cairns, and G. Webb (1996), Interstellar pickup ions and quasi-perpendicular shocks: Implications for the termination shock and interplanetary shocks, *J. Geophys. Res.*, *101*, 457–477.

Zilbersher, D., M. Gedalin, J. A. Newbury, and C. T. Russell (1998), Direct numerical testing of stationary shock model with low mach number shock observations, *J. Geophys. Res.*, *103*, 26,775–26,782, doi:10.1029/98JA02464.

M. Balikhin, ACSE, University of Sheffield, Sheffield S1 3JD, UK.

M. Gedalin, Department of Physics, Ben-Gurion University, Beer-Sheva 84105, Israel.

L. Ofman, CUA and NASA GSFC, Code 671, Greenbelt, MD 20771, USA.

C. T. Russell, Institute of Geophysics and Planetary Physics, University of California, Los Angeles, CA 90095, USA.